

Interaction of gaseous D atoms with alkyl halides adsorbed on Pt(111), H/Pt(111), and C/Pt(111) surfaces: Hot-atom and Eley–Rideal reactions. I. Methyl bromide

S. Wehner and J. Küppers

Citation: *The Journal of Chemical Physics* **111**, 3209 (1999); doi: 10.1063/1.479600

View online: <http://dx.doi.org/10.1063/1.479600>

View Table of Contents: <http://scitation.aip.org/content/aip/journal/jcp/111/7?ver=pdfcov>

Published by the [AIP Publishing](#)

Articles you may be interested in

[Quasiclassical study of Eley–Rideal and hot atom reactions of H atoms with Cl adsorbed on a Au\(111\) surface](#)
J. Chem. Phys. **122**, 074705 (2005); 10.1063/1.1851498

[Interaction of gaseous D atoms with alkyl halides adsorbed on Pt\(111\), H/Pt\(111\), and C/Pt\(111\) surfaces: Hot-atom and Eley–Rideal reactions. III. Isopropyl iodide](#)
J. Chem. Phys. **111**, 3225 (1999); 10.1063/1.479602

[Interaction of gaseous D atoms with alkyl halides adsorbed on Pt\(111\), H/Pt\(111\), and C/Pt\(111\) surfaces: Hot-atom and Eley–Rideal reactions. II. Ethyl iodide](#)
J. Chem. Phys. **111**, 3218 (1999); 10.1063/1.479601

[Interaction of gaseous D atoms with CH₃I adsorbed on Pt\(111\), H/Pt\(111\), and C/Pt\(111\) surfaces: From hot-atom to Eley–Rideal phenomenology](#)
J. Chem. Phys. **109**, 294 (1998); 10.1063/1.476508

[Eley–Rideal and hot-atom reaction dynamics of H\(g\) with H adsorbed on Cu\(111\)](#)
J. Chem. Phys. **107**, 6420 (1997); 10.1063/1.474302



Interaction of gaseous D atoms with alkyl halides adsorbed on Pt(111), H/Pt(111), and C/Pt(111) surfaces: Hot-atom and Eley–Rideal reactions.

I. Methyl bromide

S. Wehner

Experimentalphysik III, Universität Bayreuth, 95440 Bayreuth, Germany

J. Küppers^{a)}

Experimentalphysik III, Universität Bayreuth, 95440 Bayreuth, Germany and Max-Planck-Institut für Plasmaphysik (EURATOM Association), 85748 Garching, Germany

(Received 16 February 1999; accepted 6 May 1999)

The interaction of gaseous D atoms with methyl bromide molecules adsorbed on Pt(111), hydrogen saturated Pt(111), and graphite monolayer covered Pt(111) surfaces was studied in order to elucidate the reaction mechanisms. The reaction kinetics at 85 K surface temperature were measured as a function of the methyl bromide precoverage by monitoring reaction products simultaneously with D atom exposure. On all substrates incoming atoms abstract the methyl group from adsorbed CH₃Br via gaseous CH₃D formation. In the monolayer regime of CH₃Br/Pt(111) pure hot-atom phenomenology was observed in the rates. At multilayer targets the fluence dependence of the kinetics gets Eley–Rideal-like. With coadsorbed H present, the reaction of D with adsorbed methyl bromide revealed in addition to CH₃D a CH₄ product. This and simultaneous abstraction of adsorbed H via gaseous HD and H₂ products clearly demonstrates that hot-atom reactions occur. At CH₃Br adsorbed on a graphite monolayer on Pt(111) the abstraction kinetics of methyl was found to agree with the operation of an Eley–Rideal mechanism. These observations are in line with the expectation that hot-atoms do not exist on a C/Pt(111) surface but on Pt(111) and H/Pt(111) surfaces. The methyl abstraction cross-sections in the monolayer regime of methyl bromide were determined as about 0.25 Å², irrespective of the nature of the substrate. This value is in accordance with direct, Eley–Rideal or hot-atom reactions. © 1999 American Institute of Physics.

[S0021-9606(99)71329-2]

I. INTRODUCTION

Reactions between gaseous atoms and adsorbed species are currently described by the Eley–Rideal (ER)¹ and hot-atom mechanisms (HA).² Atomic beam/laser spectroscopy studies performed on abstraction of D adsorbed on Cu(111) surfaces by H atoms towards HD revealed that the HD product carries the available reaction energy,³ in line with the operation of either mechanism. On the other hand, abstraction of D(ad) ((H(ad)) by gaseous H(D) on Ni(100),⁴ Pt(111),^{5,6} Pt(110),⁷ Pt(100),⁸ and Cu(111)⁹ surfaces, investigated through direct product detection, revealed HD kinetics which are not compatible with the operation of ER mechanisms. Furthermore, in these studies as well as in a previous investigation on Ni(110),¹⁰ homonuclear species, D₂(H₂), were obtained as reaction products which are unexpected in an ER scenario.

Model calculations of the HD and D₂ kinetics in H→D(ad) reactions were performed recently¹¹ based on three assumptions:

- (i) H atoms impinging at empty or H occupied sites on a surface get hot H* atoms.

- (ii) H atoms impinging at D occupied sites get hot H* atoms with probability $1 - p_b$ and generate hot D* atoms with probability p_b .
- (iii) Hot H* and D* atoms travel across the surface and stick at empty sites with probability p_s and react at occupied sites with probability p_r .

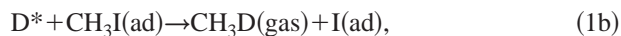
Within this purely HA based model, measured HD and D₂ kinetics on Ni(100), Pt(111), and Cu(111) surfaces could be reproduced surprisingly well at fixed p_b by variation of the ratio p_r/p_s from 1 (Cu) over 0.1 (Ni) to 0.01 (Pt). The branching probability p_b served to adjust the yield of homonuclear products.

Significance of HA based processes in atom–adsorbate reactions was previously concluded from molecular dynamics calculations, H→D/Si(100) (Ref. 12) and H→D/Cu(111) (Ref. 13). The origin of hot atoms in these calculations is the strong attractive atom–surface potential and the inability of the impinging atoms to transfer their kinetic energy to the substrate in collisions with heavy surface atoms. This feature was already stressed in the original work on the HA mechanism by Harris and Kasemo.²

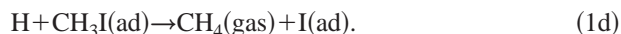
HA type processes are not restricted to the H–D (ad) interaction. A study on the reactions of gaseous H(D) with methyl iodide (CH₃I, CD₃I) adsorbed and coadsorbed with D(H) on Ni(100) surfaces¹⁴ revealed products which could

^{a)}Author to whom correspondence should be addressed. Electronic mail: kueppers@ipp.mpg.de, kueppers@uni-bayreuth.de

only originate through reaction pathways in which hot atoms were involved. As examples, for the reaction $\text{H} \rightarrow \text{D}/\text{CH}_3\text{I}$ on Ni(100) these products were in addition to the expected CH_4 product CH_3D and D_2 which occur through the HA processes



with hot atoms (stared species) as the actual reacting species. The occurrence and kinetics of the CH_3D and D_2 products contradict the operation of an ER mechanism which, for the addressed case, would predict only a CH_4 product through

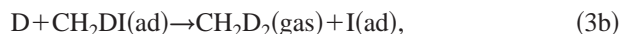
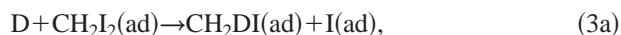


These investigations revealed that products and kinetics of atom-adsorbate reactions on metallic substrates cannot be explained by the ER scenario in a satisfactory manner. In contrast, a recent study on the reactions between D atoms and methyl iodide adsorbed on graphite monolayer covered Pt(111) surfaces, C/Pt(111),¹⁵ revealed kinetics of the CH_3D reaction product which are strictly according to the operation of an ER mechanism. The measurements utilized simultaneous detection of the methane product during application of a D atom flux Φ which was applied at the adsorbate as a step function of time t , i.e., $\Phi = 0$ at $t < 0$ and $\Phi = \text{const.}$ at $t \geq 0$. The gas phase methane product rate, $d[\text{CH}_3\text{D}]/dt$, was found to precisely match the rate predicted by the solution of the kinetic equation which describes the reaction in an ER scheme:

$$d[\text{CH}_3\text{D}]/dt = [\text{CH}_3\text{I}]_0 \sigma \Phi \exp(-\sigma \Phi t), \quad (2)$$

with $[\text{CH}_3\text{I}]_0$ as initial coverage of methyl iodide on C/Pt(111), σ as reaction cross-section, and $\Phi(t)$ as specified above. The reaction cross-section σ was determined from the measured kinetics as 0.7 \AA^2 . This magnitude of σ is in accordance with the locality of the reaction event in an ER scenario.

The conclusion that on nonmetallic C/Pt(111) substrates atom-adsorbate reactions proceed according to the ER mechanistic description gained support by a study on the reactions between D atoms and methylene iodide (CH_2I_2) adsorbed on C/Pt(111) surfaces.¹⁶ The reaction sequence



can be interrupted after the first reaction step (3a) by performing the reaction at substrate temperatures above the methyl iodide desorption temperature and methyl iodide then is the gaseous reaction product. Alternatively, below the methyl iodide desorption temperature, the second reaction step (3b) also occurs and methane is the final product. The rates of both gas phase products, CH_2DI at high T and CH_2D_2 at low T, can be calculated from the kinetic equations with the assumption that ER-type mechanisms with two cross-sections σ_1 [3(a) towards CH_2DI] and σ_2 [3(b) towards CH_2D_2] apply. The measured kinetics were found in excellent agreement with calculated rates and cross-sections σ_1

$= 2.4 \text{ \AA}^2$, $\sigma_2 = 1 \text{ \AA}^2$ were deduced. This magnitude of cross-sections is expected if ER mechanisms operate in these reactions.

The observation of HA-type processes on metal surfaces and ER type processes on C/Pt(111) is in line with the fact that a graphite monolayer on Pt(111) removes the strong attractive atom-surface interaction since the potential between the basal plane of graphite and H is weak. Accordingly, the most important requirement for the generation or existence of hot atoms on the surface is missing on C/Pt(111) substrates and HA mechanisms are ruled out.

The present study was performed to further investigate the elementary steps in reactions between gas phase deuterium atoms and adsorbed alkyl halides. Target molecule methyl bromide was selected since it allows to study the influence of the methyl-halide binding energy by comparison with reactions of methyl iodide. In order to confirm the role of the substrate, metallic vs. nonmetallic, the reactions were investigated on Pt as well as on H and graphite covered Pt surfaces.

II. EXPERIMENT

The experiments were carried out in the UHV system used for the previous study on the D/adsorbed methyl (methylene) iodide reactions.^{15,16} The system is equipped with LEED/AES instrumentation and a setup for atom/adsorbate reaction studies. D atoms were generated in an atom source built according to a published design¹⁷ and characterized recently with respect to its efficiency for hydrogen atom generation.¹⁸ It consists of a W tube which is heated at its front end by electron impact and connected at its cooled back end to a deuterium gas supply. The atom flux delivered by this source was calculated from the gas flow through the tube, tube front temperature (1950 K), and the $\text{D}_2/2\text{D}$ equilibrium data. D atom fluxes are given below in units of monolayers s^{-1} with respect to the Pt(111) surface atom density, $1 \text{ Mls}^{-1} = 1.5 \times 10^{15} \text{ D cm}^{-2} \text{ s}^{-1}$. The atom source is incorporated into a cylindrical, differentially pumped separate vacuum system (source chamber) which sticks into the main chamber. The source chamber has a front aperture which can be closed by a mechanical shutter. For reaction measurements, the sample with a well defined adsorbate coverage was placed in front of the closed aperture. Opening of the shutter defined the reaction start and reaction products were monitored subsequently by a quadrupole mass spectrometer (QMS) located in the source chamber. Typically, partial pressures in 15–20 preselected amu channels were multiplexed with appropriate sensitivities. Through fragmentation analysis unambiguous product identification was possible. An optical link between the QMS electronics and the PC which controlled the experiment provided the high data transfer rate required for fast multiplexing. Since the setup resembles a pumped reactor, partial pressures monitored by the QMS are proportional to reaction or desorption rates of the respective species at or from the surface. With the atom source switched off the arrangement served for thermal desorption (TD) spectroscopy.

A disk-shaped Pt(111) single crystal was spot-welded between two Ta wires which were attached to two Cu rods

fixed at the bottom of a small cryostat. Via ohmic heating and LN₂ cooling of the Ta wires, sample temperatures between 85 and 1200 K could be installed. The sample temperature was monitored and regulated by a PC-controlled programmer connected to a Ni/CrNi thermocouple which was welded to the back of the crystal.

Methyl bromide was obtained from Merck (99%) and purified by freeze-pump cycles in a gas handling line. Methyl bromide exposures given below were obtained from uncorrected ion gauge readings. The sample was cleaned by sputtering and annealing in oxygen. Graphite monolayers were deposited on the Pt(111) surface by repeated chemical vapor deposition (CVD) of ethane and subsequent annealing at 1200 K until complete suppression of hydrogen adsorption on the surface indicated that there were no Pt patches uncovered by C. A STM study has shown that at that stage the Pt surface is covered by one monolayer high graphite islands.¹⁹ These islands withstand repeated heating to 1000 K and are stable against H atom impact since they are only hydrogenated at their boundaries and do not erode chemically.²⁰

III. RESULTS

A. Methyl bromide desorption

In order to establish the monolayer regimes of methyl bromide on clean as well as on H and C covered Pt(111) surfaces, thermal desorption measurements were performed on the different substrates. Figure 1 shows spectra measured in the monolayer and multilayer regimes after exposure of CH₃Br at 85 K substrate temperature. The spectra measured on Pt(111) are in excellent agreement with those published recently by French and Harrison.²¹ Monolayer chemisorbed methyl bromide desorbs between 120 and 240 K, and above 25 L exposure simultaneous growth of multilayer and monolayer features is observed. On C/Pt(111) surfaces the chemisorbed state is replaced by a weaker bound state which desorbs via a zero-order process around 125 K. This desorption order indicates that methyl bromide prefers to adsorb in islands on the C/Pt(111) surface. Methyl bromide multilayer features start to grow a little earlier than at completion of the monolayer. On deuterium saturated Pt(111) surfaces the chemisorbed monolayer state of methyl bromide on Pt(111) is also replaced by a weaker bound state which desorbs around 128 K. Its desorption features indicate a zero-order process. The desorption temperatures of the multilayer species on Pt(111), D/Pt(111), and C/Pt(111) surfaces are very similar, as expected. Integration of the desorption spectra revealed identical uptake as a function of methyl bromide exposure at the three substrates and suggest a constant sticking coefficient throughout the exposure regime investigated here. The upper part of Fig. 1 displays the relation between exposure and coverage obtained by setting the monolayer capacity on C/Pt(111) surfaces as unity.

Thermal desorption was monitored simultaneously in the amu 96 (CH₃⁸¹Br), amu 94 (CH₃⁷⁹Br), and amu 15 (CH₃ fragment) channels. The respective spectra were identical after proper scaling, as expected. Signals in other channels monitored during TD spectroscopy, amu 2, 3, 4, 14, 18, 28

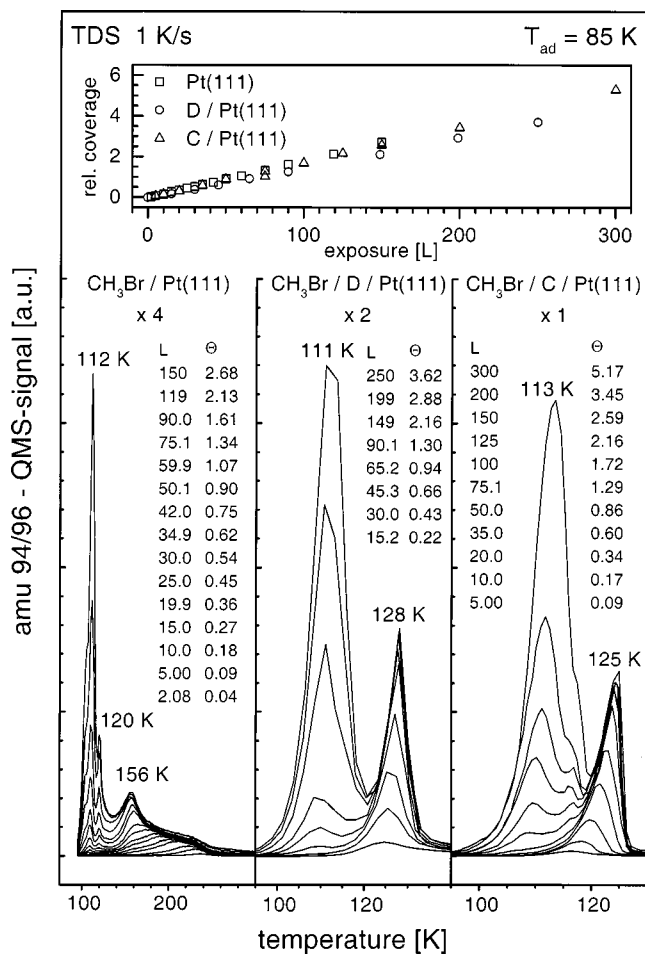


FIG. 1. Thermal desorption spectra of methyl bromide adsorbed on Pt(111) (left), deuterium covered Pt(111) (middle), and graphite monolayer covered Pt(111) (right). Adsorption temperature 85 K. Note the scale factors for each panel. The spectra are stacked according to the respective lists of exposures in L (1 L = 10⁻⁶ Torr × sec). The relative coverages listed in each panel are normalized with respect to the saturated monolayer coverage on C/Pt surfaces. The top panel illustrates the relation between coverage and exposure.

confirmed that the adlayers had been prepared with the required purity.

On Pt(111) surfaces, a small methane desorption feature at 290 K indicates that a few percent of adsorbed methyl bromide decomposed. Decomposition of methyl bromide was virtually absent on C/Pt(111) and H/Pt(111), in line with its weak bonding to those substrates. The apparent modification of ad molecule Pt(111) interactions through sandwiched C or H monolayers was observed earlier with several adsorbates, benzene,²² methyl iodide,¹⁵ methylene iodide,¹⁶ isopropanol,²³ propene oxide.²⁴ This modification is indicative of the effective shielding of the metal by H and C overlayers.

For all three adsorbate systems it proved impossible to prepare pure monolayers without multilayer contributions by overdosing the surfaces and subsequently (even repeatedly) flashing the sample to an appropriate temperature in the range 100 to 120 K. Therefore, abstraction experiments were performed with as-prepared adsorbed layers at 85 K.

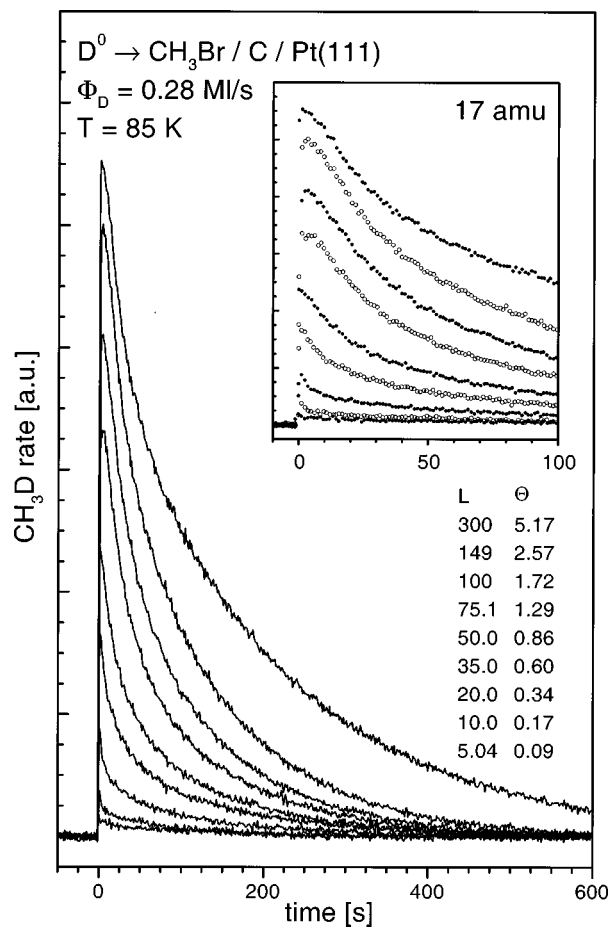


FIG. 2. Rates of CH_3D formation during directing D atoms at methyl bromide adsorbed on C/Pt(111) surfaces. Exposures and coverages listed specify the initial condition of the CH_3Br adlayers. The D flux was started at $t=0$ and kept constant thereafter. The inset emphasizes the early reaction period.

B. Abstraction from methyl bromide on C/Pt(111)

Exposure of gaseous D atoms to methyl bromide adsorbed on C/Pt(111) surfaces revealed CH_3D as the only gaseous product, identified through its tabulated fragmentation pattern in the amu 17, amu 16, and amu 15 channels.²⁵ Figure 2 illustrates the evolution of the CH_3D rate with reaction time for increasing methyl bromide coverages established prior to reaction. The substrate temperature was fixed at 85 K and the atom flux held constant at 0.28 MI s^{-1} during the measurements. Since the adsorption energy of methane on C/Pt(111) is very small, at 85 K reaction temperature desorption of methane is not rate limiting and the rates shown in Fig. 2 are rates of formation of CH_3D in the D/methyl bromide interaction. The reactions proceed until complete consumption of methyl groups available in methyl bromide on the surface, verified through post-reaction desorption spectra. Remaining bromine had to be removed from the surface by flashing the sample to 1000 K in order to recover clean C/Pt(111).

The reaction kinetics for different methyl bromide coverages apparent from the rates shown in Fig. 2 exhibit common features. At reaction start (opening of the shutter) the methane rates jump to their maximum values and fall off

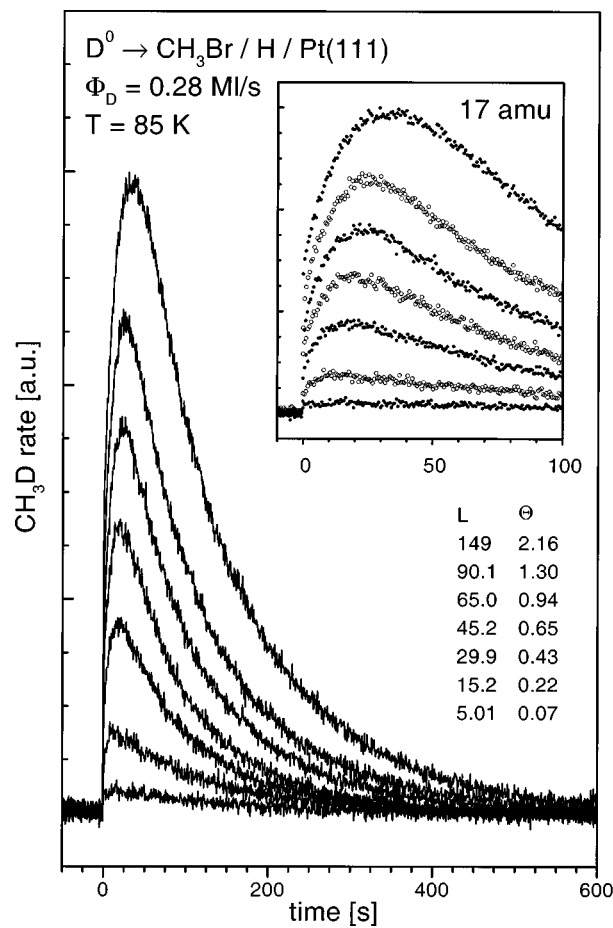


FIG. 3. Rates of CH_3D formation during directing D atoms at methyl bromide adsorbed on H covered Pt(111) surfaces. Other details see caption of Fig. 2.

thereafter. The initial rate jumps as well as the amounts of CH_3D produced during subsequent reaction increase with increasing methyl bromide coverage. The inset in Fig. 2 illustrates the measured rates on an expanded time-scale which emphasizes the initial period of the reaction and clarifies that rate jumps occur at reaction start and not continuous rate increases from zero.

CH_3D formation rates measured with other D atom fluxes, up to 0.48 MI s^{-1} , revealed identical kinetics as those shown in Fig. 2 with the time axis rescaled to a fluence (flux*time) axis and proper adjustment of the rate scale. CH_2D_2 and DBr products were never detected.

C. Abstraction from methyl bromide on H/Pt(111)

Reaction measurements with coadsorbed H and methyl bromide were performed at Pt(111) surfaces which were initially saturated with H via exposure of 1000 L H_2 at 85 K followed by subsequent installation of a required methyl bromide coverage by exposing CH_3Br to the H covered surface. The kinetics of CH_3D formation during D atom exposure measured at increasing methyl bromide coverages are shown in Fig. 3. Like on C/Pt(111) surfaces, methyl groups in adsorbed methyl bromide are completely consumed during reaction. The rates jump at reaction start to values which increase with increasing methyl bromide coverage.

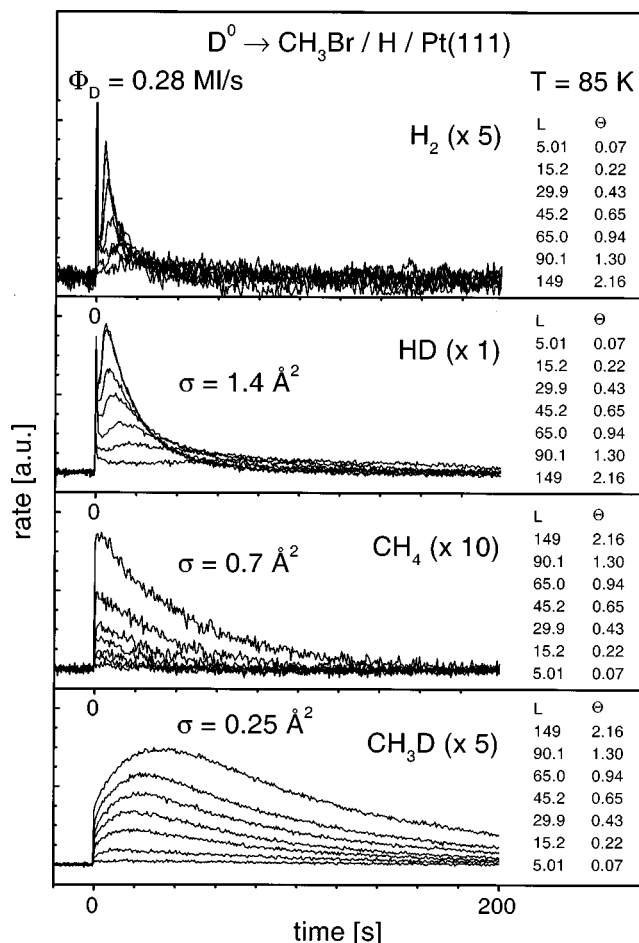


FIG. 4. Rates of H_2 , HD, CH_4 , and CH_3D formation during directing D atoms at methyl bromide adsorbed on H covered Pt(111) surfaces. Note the different stacking order of the rate curves as a function of the methyl bromide coverage indicated by the exposures and coverages. The spikes at $t = 0$ in the H_2 and HD rates are due to friction desorption caused by the shutter plate sliding along the front face of the source chamber.

Subsequently, in an early reaction period, the rates grow, achieve maxima at reaction times which increase with methyl bromide coverage, and fall off in late reaction periods. The inset in Fig. 3 emphasizes these features. A growth of the CH_3D rate in the early reaction period during which the methyl bromide coverage decreases contradicts the Eley-Rideal reaction mechanism and suggests the presence of a more complex reaction scenario.

The collection of kinetic data shown in Fig. 4 confirms this expectation. In addition to CH_3D , H_2 , HD, and CH_4 are reaction products of the D-methyl bromide H/Pt(111) interaction, and each product occurs with its own kinetics. The occurrence of HD and H_2 is required since from the investigations mentioned in the introduction, it is known that the D/H(ad) interaction results in the release of these products. Furthermore, a CH_4 product is not unexpected in view of the earlier study on Ni(100).¹⁴ The yield and kinetics of the four species will be analyzed in detail below.

D. Abstraction from methyl bromide on Pt(111)

CH_3D , identified through its fragmentation pattern, was the only gaseous product detected during the interaction be-

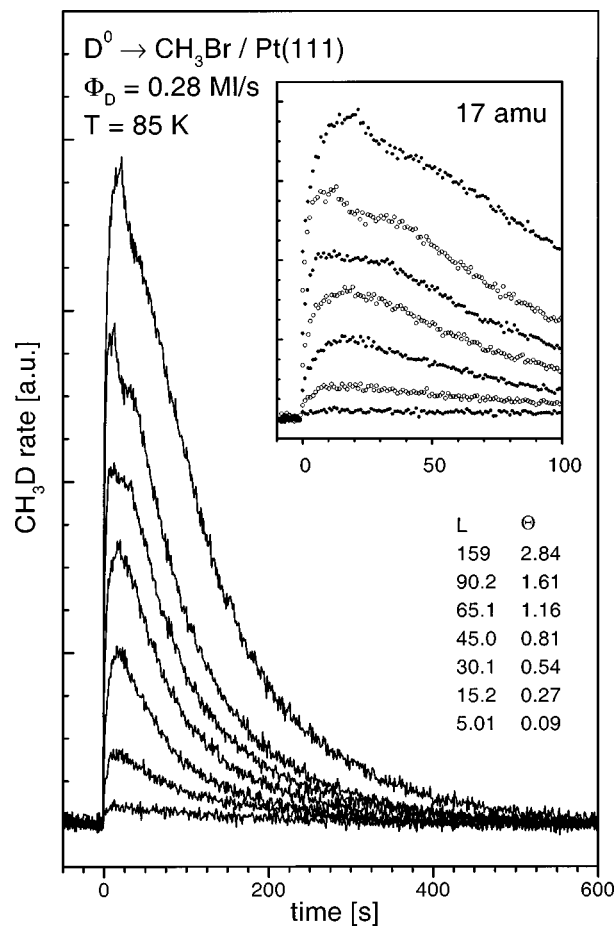


FIG. 5. Rates of CH_3D formation during directing D atoms at methyl bromide adsorbed on Pt(111) surfaces. Other details see caption of Fig. 2.

tween D and adsorbed methyl bromide on Pt(111). The measured rates are shown in Fig. 5. Similar to the kinetics of the methane product in the reaction of D with coadsorbed H/ CH_3Br , at reaction start the rates exhibit a rate step and a subsequent increase. After achieving a maximum the rates fall to zero in a late reaction period. Post-reaction desorption spectra confirmed that methyl abstraction was complete.

IV. DISCUSSION

The reactions of D atoms with adsorbed methyl bromide revealed CH_3D as product, irrespective of the substrate, Pt(111), H/Pt(111), or C/Pt(111). In view of previous results on the abstraction of methyl by H from methyl iodide adsorbed on Cu(111) (Ref. 26) and Ni(100) (Ref. 14) surfaces, this is not surprising. The CH_3-Br bond strength, 293 kJ/mol,²⁷ is only a little bigger than that of CH_3-I , 234 kJ/mol,²⁸ and the CH_3-H bond strength of 438 kJ/mol (Ref. 27) makes the methyl abstraction reaction substantially exothermic even if the Maxwellian distribution of D atom energies delivered from the heated source, centered at about 20 kJ/mol, is not taken into account. There is a further contribution to the reaction energy from the gain in adsorption energy of Br vs CH_3Br .

A CH_2D_2 product was never observed, indicating that abstraction of H by D from the methyl group of CH_3Br followed by subsequent hydrogenation back to CH_2DBr is

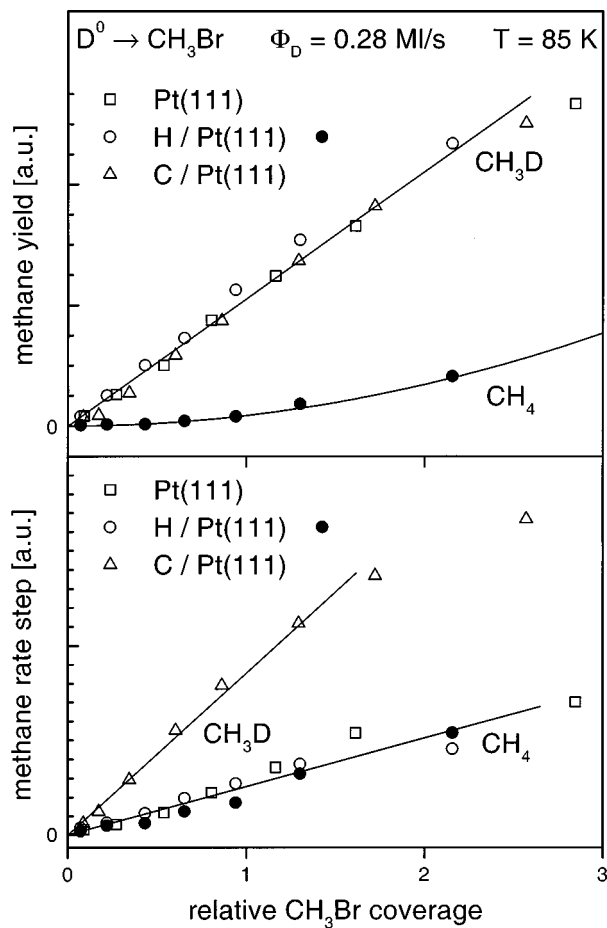


FIG. 6. Reaction yields of CH_3D and CH_4 deduced from integrated rates of methane as a function of initial methyl bromide coverage determined through TDS (top). Rate steps of CH_3D and CH_4 as a function of initial methyl bromide coverage (bottom).

much slower than the abstraction of the methyl group from methyl bromide. The same was observed in the D-methyl iodide interaction. With adsorbed CH_3Cl , however, the abstraction cross-section of H from the methyl group is comparable to abstraction of the methyl group.²⁹ The stronger $\text{CH}_3\text{-Cl}$ bond energy as compared to $\text{CH}_3\text{-Br}$ makes this feature plausible.

As mentioned, during abstraction all methyl groups of adsorbed methyl bromide available on the surface were consumed. The methane yields obtained from integrated rates are displayed in Fig. 6 (top) as a function of the initial bromide coverage. On the three substrates the CH_3D yield is proportional to this relative coverage. Therefore, the energy set free upon reaction is not channelled to the adsorbate or substrate since in that case some of the adsorbed methyl bromide would desorb and not be available for reaction. This would induce a nonlinearity between the methane yield and the coverage of methyl bromide present on the surface at reaction start.

The kinetics of the $\text{D}\rightarrow\text{CH}_3\text{Br}/\text{C}/\text{Pt}(111)$ reaction is simple to analyze. Figure 6 (bottom) shows that the rate steps deduced from Fig. 2 are proportional to the coverage if one restricts to the coverage range below $\Theta=2$. Therefore, an essential condition for the ER mechanism, proportionality

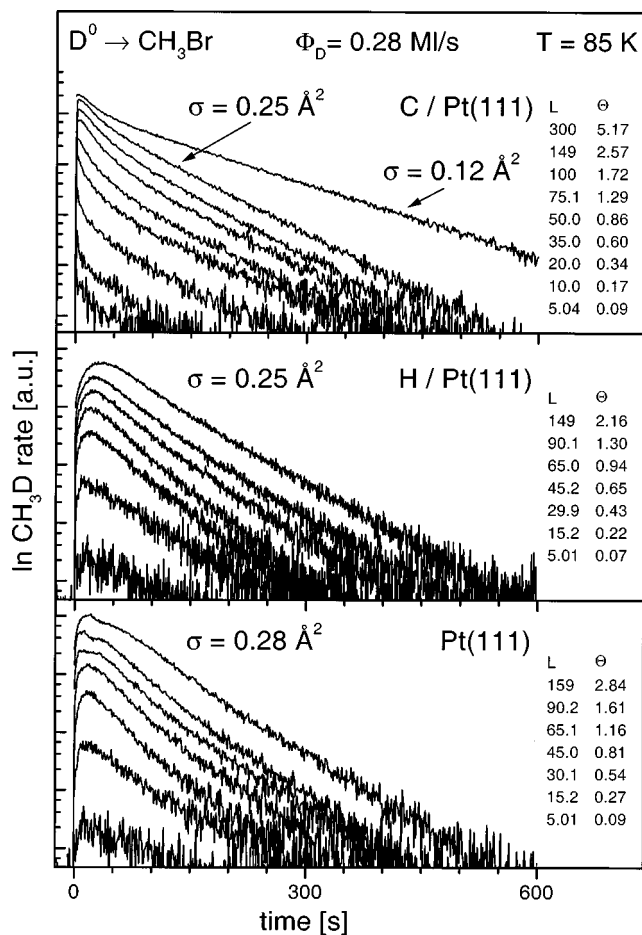


FIG. 7. Logarithmic representation of the CH_3D rates shown in Figs. 2, 3, and 5. C/Pt(111) (top), H/Pt(111) (middle), Pt(111) (bottom).

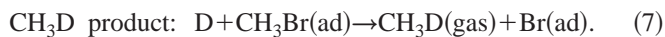
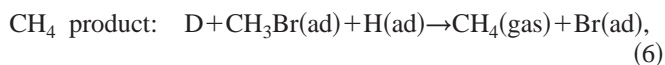
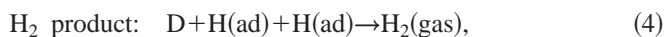
between rate step and initial coverage of the surface reactant, as expressed in Eq. (2), is fulfilled. A logarithmic plot of the CH_3D rates against reaction time is shown in Fig. 7 (top). Excluding the initial 50 s of reaction time, the logarithms of the rates decrease linearly with reaction time, which makes the rate decay proportional to $\exp(-\sigma\Phi t)$, as required by ER. The scaling of the rates with the fluence Φt was confirmed by the flux dependence of the rates. With this requirement fulfilled, the extraction of a cross-section from the logarithmic rates is justified. The cross-section derived from Fig. 7(top) is $\sigma=0.25 \text{ \AA}^2$. This value is in the range expected for ER type reactions and significantly lower than that measured in abstraction of methyl from methyl iodide on C/Pt(111), $\sigma=0.7 \text{ \AA}^2$.¹⁵ Energetic and steric reasons like exothermicity, target molecule size, and its orientation on the surface might be the origin of these different cross-sections. The fact that the rate steps are proportional to the coverage not only in the monolayer range but also for the second layer suggests that incoming D atoms can access monolayer species for reaction even through the second layer. This is plausible since CH_3Br molecules are loosely packed due to their large dipole moment.

The topmost curves in Fig. 2 and Fig. 7 (top) correspond to a thick methyl bromide multilayer, $\Theta=5$. The cross-section derived from the exponential CH_3D rate decay is only 0.12 \AA^2 and the rate step at that coverage is much

smaller than expected by extrapolation from the monolayer regime. The observation that abstraction from thick multilayers exhibits a smaller cross-section than those characteristic for monolayers was also made in abstraction from adsorbed CH_3I and its isotope analogs.¹⁵

The steep slope of the logarithmic rates in the first 50 s of reaction time in Fig. 7(top) suggests that initially abstraction is faster than at later times. Since abstraction from multilayers exhibits a smaller cross-section than from monolayers, initial faster abstraction cannot originate from the multilayer components in the adsorbed methyl bromide mono- and bilayers.

Whereas on C/Pt(111) the reaction of D with methyl bromide can be assigned as an ER reaction, the products and their kinetics shown in Fig. 4 clearly contradict the operation of an ER mechanism in abstraction from CH_3Br on the H/Pt(111) surface. In reading the kinetic data shown in Fig. 4, it has to be noticed that the H_2 and HD rates refer (from top to bottom) to increasing methyl bromide coverage, whereas the methane rates refer (from top to bottom) to decreasing methyl bromide coverage. The marked differences in the decay of the rates suggests individual pathways for the various products. According to the products observed, the overall reactions occurring with mixed H/ CH_3Br adlayers are:



Reactions (4) and (5) were investigated previously in this laboratory by studies of the $\text{H} \rightarrow \text{D}(\text{ad})/\text{Pt}(111)$ (Ref. 5) and $\text{D} \rightarrow \text{H}(\text{ad})/\text{Pt}(111)$ (Ref. 6) interaction and were identified as hot-atom reactions. The kinetics of the H_2 and HD products in Fig. 4 agree with these earlier results and their essential characteristics were explained in a simplified hot-atom scenario by the model calculations¹¹ mentioned in the introduction. The elementary reaction steps including hot atom species behind reaction (4) are (with starred atoms specifying hot-atom species):



and behind reaction (5)



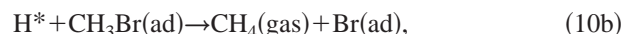
With ongoing reaction H(ad) gets replaced by D(ad) and D_2 products occur through the reaction steps



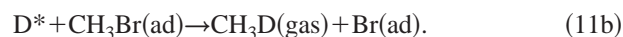
The D_2 product could not be monitored since the atom source was operated with D_2 .

Concentrating on the H_2 and HD rates in Fig. 4 with the smallest methyl bromide coverage ($\Theta = 0.07$ after 5 L methyl bromide exposure) it is apparent that these rates do not achieve their maximum values right at reaction start, which they would if ER-type processes would occur. Since through exposure of molecular H_2 to Pt(111) surfaces only a coverage of about 0.7 is achieved³⁰ there are still empty sites available on the surface. Hot-atom species generated through reactions (8a) and (9a) which travel across the surface can stick at these empty sites and are unavailable for reaction (8b) or (9b). Therefore, the HD and H_2 rates at reaction start do not achieve their maximum values. During the early reaction period after reaction start, through hot-atom sticking events, the number of empty sites gets smaller and hot-atom reactions (8b) and (9b) get more probable. By this effect, the rates of H_2 and HD increase. They achieve maximum values if the number of empty sites cannot decrease any more since stationary conditions with respect to the H+D coverage is reached. Behind its maximum the HD rate decreases exponentially, as required for a quasifirst-order reaction, scheme (9a), (9b). The cross-section deduced from the rate decay of HD is $\sigma = 1.4 \text{ \AA}^2$, in good agreement with the earlier result.¹⁶ The H_2 rate decays faster since it is a second-order process with respect to the coverage of H(ad), see reaction scheme (8a), (8b).

Approaching higher methyl bromide coverages, the H_2 and HD rates decrease since adsorbed H is consumed by the reactions towards CH_4 , reaction (6), and D in reactions towards CH_3D , reaction (7). These competing reactions also cause the rate maxima of the H_2 and HD rates to shift to later reaction time with increasing methyl bromide coverage. The phenomenology of the methane rates suggest the following pathways via hot-atoms to CH_4 :



and to CH_3D :



It is clear that CH_4 can only occur through a hot-atom mechanism. Through reactions (10a) and (10b) its rate assumes its maximum right at reaction start, because at that moment the coverage of H(ad) at the surface is bigger than at any later time. The consumption of H(ad) towards H_2 and HD products effectively competes with CH_4 formation. Therefore, the rates of CH_4 decrease continuously with reaction time and the CH_4 yields are much smaller than that of CH_3D , compare Fig. 6. The reaction sequence (10a), (10b) allows to describe CH_4 production through a quasifirst-order rate law, and a reaction cross-section of $\sigma = 0.7 \text{ \AA}^2$ was obtained.

The CH_3D kinetics is also not according to an ER mechanism. Its rate jumps at reaction start since step (11a) provides hot D^* species required for reaction (11b). At ongoing reaction, through depletion of H(ad), the formation of CH_4 and HD becomes less competitive and the CH_3D rate increases. Through the decrease of methyl groups available

for reaction a rate maximum is obtained. In the late reaction period adsorbed hydrogen is replaced by adsorbed deuterium and the reaction step



replaces reaction (11a) for providing the hot D^* species necessary for reaction.

The branching towards H^* or D^* in competing steps (10a) and (11a) favors the production of D^* , and therefore more CH_3D molecules than CH_4 molecules are formed. This preference for formation of hot species from the impinging atom rather than from the adsorbed atom is generally observed:⁴⁻¹⁰ in $D \rightarrow H(\text{ad})$ reactions, HD is the major product and H_2 only in the percent range. Likewise, in $H \rightarrow D(\text{ad})$ reactions, HD product molecules outnumber D_2 molecules.

The rate steps of CH_4 and CH_3D are quite similar as depicted in Fig. 6 (bottom). This illustrates the effectivity of HD formation, since at reaction start adsorbed H and adsorbed CH_3Br compete for reaction with hot D^* atoms.

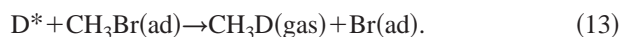
It is not surprising that the complex reaction scenario in the early reaction period causes the logarithmic plot of the CH_3D rates in Fig. 7 (middle) to exhibit a clear linear decrease only in the late period. The cross-section deduced in this period for the abstraction of methyl from methyl bromide by D is $\sigma = 0.25 \text{ \AA}^2$, very similar to the value obtained above at the C/Pt(111) surface. This is expected since for the abstraction process itself it should not matter very much whether the substrate is a metal or not. The value 0.25 \AA^2 is smaller than the cross-sections towards HD (1.4 \AA^2) and CH_4 (0.7 \AA^2) and explains why the CH_3D product exhibits such a slow decay, see Fig. 4.

With the reaction between D atoms and adsorbed methyl bromide on C/Pt(111) and H/Pt(111) surfaces identified as Eley-Rideal or hot-atom reactions, the discussion of the results measured with methyl bromide on Pt(111) is quite simple. Since the substrate is metallic, the following reactions at reaction start are expected:

Hot-atom generation on empty sites:



Hot-atom reaction with adsorbed CH_3Br :



Hot-atom sticking:



At later times in addition the following reactions occur:

Hot-atom generation on D occupied sites:



Hot-atom reaction with adsorbed D:



The combination of reactions (12) and (13) should produce a rate step at reaction start. Reaction (14) is competitive to (13) and affects the step height. At ongoing reaction empty sites are filled and the competition of step (14) gets less important.

Through reaction (15) more hot D^* atoms are made available for reaction and the CH_3D rate increases. It achieves a maximum when an optimum condition is achieved concerning the concentration of adsorbed methyl bromide molecules and rate of available hot D^* atoms. At ongoing reaction, through consumption of the methyl groups, the CH_3D rate decreases. Comparing with Fig. 5 it is seen that this pattern is verified by the experiments in the methyl bromide monolayer coverage range where multilayer contributions can be neglected, exposures less than 65 L. At higher exposures multilayers develop and shield the metal from the incoming D atoms. An ER-type mechanism should then contribute, indicated by a shift of the rate maximum towards the reaction start. Checking with the kinetics in Fig. 5 this expectation is confirmed. The CH_3D yield and rate step in Fig. 6 are as expected from the previous discussion.

The cross-section revealed from the logarithmic rate plot in Fig. 7 (bottom), restricted to the late reaction period, is $\sigma = 0.28 \text{ \AA}^2$. This value is close to those deduced above for the other substrates and its magnitude is as expected. The topmost logarithmic rate in Fig. 7 (bottom) indicates that with increasing thickness of the multilayers the cross-section gets smaller, as already seen in the top curve in Fig. 7 (top). Since its corresponding coverage is much bigger than that to which Fig. 7 (bottom) refers, this feature is more clearly seen there.

In the above discussion the concepts of ER and HA mechanisms were successfully applied to abstraction of methyl from methyl bromide adsorbed in mono- and multilayers on various substrates. Products and the phenomenology of their kinetics could be rationalized in a qualitative but satisfactory manner using the simple principles developed earlier.^{5,6,11} According to these principles, on substrates with weak atom-surface interaction, atom-adsorbate reactions should proceed via ER mechanisms, whereas strong atom-surface interaction leads to HA mechanisms. In the latter case, consequences of hot-atom generation and the interplay between hot-atom sticking and reaction induces products and kinetics which are unexpected in an ER scenario. The experimental foundation for support of the general applicability of these principles is still rather limited since only a few studies exist from which satisfactory kinetic information on atom-adsorbate reactions is available. However, the present study revealed results which are in line with expectations from these principles.

V. CONCLUSIONS

The interaction of D atoms with methyl bromide adsorbed on Pt(111), hydrogen covered Pt(111), and graphite monolayer covered Pt(111) surfaces leads to CH_3D as gaseous product, with Br remaining on the surface. The kinetics of the gaseous products were used to identify the reaction mechanisms leading to these products. On C/Pt(111) pure Eley-Rideal phenomenology was observed. On H/Pt(111), products like H_2 and CH_4 occur simultaneously with CH_3D and HD, indicative of hot-atom reaction mechanisms. On Pt(111) the kinetics of the CH_3D product also is in line with hot-atom mechanisms. The cross-sections for CH_3D forma-

tion are about 0.25 \AA^2 , significantly smaller than that for abstraction of methyl from adsorbed methyl iodide, 0.7 \AA^2 , and probably due to the higher methyl-halide bond energy in methyl bromide. Eley-Rideal phenomenology on C/Pt(111) surfaces and hot-atom phenomenology on H/Pt(111) and Pt(111) are in line with expectations drawn from role of a metallic substrate in atom-adsorbate reactions.

ACKNOWLEDGMENT

Support of this research by the Deutsche Forschungsgemeinschaft is gratefully acknowledged.

- ¹D. D. Eley and E. K. Rideal, *Nature (London)* **146**, 401 (1940).
- ²J. Harris and B. Kasemo, *Surf. Sci.* **105**, L281 (1981).
- ³C. T. Rettner and D. J. Auerbach, *J. Chem. Phys.* **104**, 2732 (1996).
- ⁴Th. Kammler, J. Lee, and J. Küppers, *J. Chem. Phys.* **106**, 7362 (1997).
- ⁵S. Wehner and J. Küppers, *J. Chem. Phys.* **108**, 3353 (1998).
- ⁶S. Wehner and J. Küppers, *Surf. Sci.* **411**, 46 (1998).
- ⁷Th. Biederer, Th. Kammler, and J. Küppers, *Chem. Phys. Lett.* **286**, 15 (1998).
- ⁸Th. Zecho, B. Brandner, and J. Küppers, *Surf. Sci.* **418**, L26 (1998).
- ⁹Th. Kammler and J. Küppers (unpublished).
- ¹⁰G. Eilmsteiner, W. Walkner, and A. Winkler, *Surf. Sci.* **352-354**, 263 (1996).
- ¹¹Th. Kammler, S. Wehner, and J. Küppers, *J. Chem. Phys.* **109**, 4071 (1998).
- ¹²P. Kratzer, *J. Chem. Phys.* **106**, 6752 (1997).
- ¹³B. Jackson and M. Persson, *J. Chem. Phys.* **96**, 2378 (1992); M. Persson and B. Jackson, *ibid.* **102**, 1078 (1995); M. Persson and B. Jackson, *Chem. Phys. Lett.* **237**, 468 (1995); B. Jackson and M. Persson, *J. Chem. Phys.* **103**, 6257 (1995); S. Caratzoulas, B. Jackson, and M. Persson, *ibid.* **107**, 6420 (1997).
- ¹⁴Th. Kammler and J. Küppers, *J. Chem. Phys.* **107**, 287 (1997).
- ¹⁵S. Wehner and J. Küppers, *J. Chem. Phys.* **109**, 294 (1998).
- ¹⁶S. Wehner and J. Küppers, *Chem. Phys. Lett.* **288**, 873 (1998).
- ¹⁷U. Bischler and E. Bertel, *J. Vac. Sci. Technol. A* **11**, 458 (1993).
- ¹⁸C. Eibl, G. Lackner, and A. Winkler, *J. Vac. Sci. Technol. A* **16(5)**, 1 (1998).
- ¹⁹T. A. Land, R. Michely, R. J. Behm, J. C. Hemminger, and G. Comsa, *Surf. Sci.* **264**, 261 (1992).
- ²⁰Th. Zecho, A. Horn, J. Biener, and J. Küppers, *Surf. Sci.* **397**, 108 (1997).
- ²¹C. French and I. Harrison, *Surf. Sci.* **387**, 11 (1997).
- ²²C. Lutterloh, J. Biener, K. Pöhlmann, A. Schenk, and J. Küppers, *Surf. Sci.* **352-354**, 133 (1996).
- ²³J. Biener, C. Lutterloh, A. Schenk, K. Pöhlmann, and J. Küppers, *Surf. Sci.* **365**, 255 (1996).
- ²⁴A. Dinger, C. Lutterloh, J. Biener, and J. Küppers, *Surf. Sci.* **421**, 44 (1999).
- ²⁵A. Cornu and R. Massot, *Compilation of Mass Spectral Data*, 2nd ed. (Heyden, London, 1975), Vol. 2.
- ²⁶Y.-S. Park, J.-Y. Kim, and J. Lee, *Surf. Sci.* **363**, 62 (1996); C. T. Rettner, D. J. Auerbach, and J. Lee, *J. Chem. Phys.* **105**, 10115 (1996).
- ²⁷*CRC Handbook of Physics and Chemistry*, 75th ed., edited by D. R. Lide (CRC, Boca Raton, 1994).
- ²⁸A. A. Radzig and B. M. Smirnov, *Reference Data on Atoms, Molecules, and Ions* (Springer Verlag, Berlin, 1985).
- ²⁹S. Wehner and J. Küppers (unpublished).
- ³⁰K. E. Lu and R. R. Rye, *Surf. Sci.* **45**, 677 (1974); K. Christmann, G. Ertl, and T. Pignet, *ibid.* **54**, 365 (1976); P. R. Norton, J. A. Davies, and T. E. Jackman, *ibid.* **121**, 103 (1982).